molecular pharmaceutics

Article

pubs.acs.org/molecularpharmaceutics

# Comparison of Cationic and Amphipathic Cell Penetrating Peptides for siRNA Delivery and Efficacy

Robert H. Mo, Jennica L. Zaro, and Wei-Chiang Shen*

Department of Pharmacology and Pharmaceutical Sciences, University of Southern California School of Pharmacy, Los Angeles, California 90033, United States

**ABSTRACT:** Cell penetrating peptides (CPPs) are short strands of arginine- and/or lysine-rich peptides (<30 amino acids) that use their cationic nature for efficient intracellular accumulation. CPPs have been used for small interfering RNA (siRNA) delivery by direct complexation with the siRNA anionic phosphate backbone. During this process, however, part of the CPP cationic charges are neutralized, and the resultant loss of free positive charges may substantially compromise CPP's internalization capabilities and eventually reduce siRNA delivery efficiency. The purpose of this study was to design a novel type of polyplex for siRNA delivery to overcome the CPP neutralization issue. This novel polyplex consists of three components: siRNA, 21mer oligolysine (K21) chemically modified to incorporate CPP conjugation sites (K21-PDP), and CPP delivery moiety. The siRNA was first neutralized by cationic charges of K21-PDP to form a polyplex. Then a cationic (hexaarginine, R6) or an amphipathic (model amphipathic peptide, MAP) CPP was conjugated to the polyplex. Agarose gel shift assays indicated that the siRNA could be released from the polyplex after K21-PDP degradation or polyplex dilution. Furthermore, the total intracellular internalization of these two CPP−polyplexes was studied. Compared with R6−polyplex, MAP−polyplex exhibited 170- and 600-fold greater uptake of fluorescently labeled siRNA at 1 and 6 h post-transfection, respectively. MAP−polyplex also exhibited comparable GFP silencing effects as Lipofectamine 2000 complex in Huh7.5 cells stably transfected to express GFP-light chain 3 protein, whereas R6−polyplex did not demonstrate significant silencing activity. Further studies indicated that the K21-PDP−siRNA polyplex formation and conjugation of MAP to the polyplex were essential for siRNA polyplex uptake and gene silencing. MAP−polyplex was also shown to be unaffected by the presence of 10% FBS during transfection. In addition, MAP−polyplex uptake was dependent on vesicle formation and fusion due to 70 and 54% loss of uptake at 4 and 16 °C, respectively, compared to incubation at 37 °C. Therefore, the amphipathic CPP is a more suitable carrier moiety for delivery of siRNA polyplex.

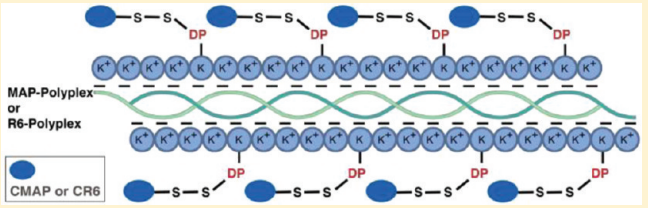


**KEYWORDS:** *Cell penetrating peptides, siRNA, siRNA delivery, oligoarginine, model amphipathic peptide, polyplex, and membrane transduction peptides*

## INTRODUCTION

RNA interference (RNAi) is an endogenous process where double stranded RNA collaborates with cytosolic proteins to inhibit gene expression by degrading target mRNA.[1] Exogenously delivered small interfering RNA (siRNA) can take advantage of this process to study gene functions,[2] elucidate molecular pathways,[3] determine prospective drug targets and develop pharmaceutical therapeutics.[4] Unfortunately, the potential of siRNA has been significantly limited by its lack of efficient intracellular delivery to the cytosol, where RNAi occurs, due to siRNA's large size, negative charge and structural fragility.[5,6] As a result, an efficient and effective delivery vehicle is essential to achieve siRNA's intracellular delivery and silencing activity. Lipofectamine 2000 is a commonly used reagent for siRNA transfection.[7] However, there are many obstacles that limit the use of Lipofectamine 2000 in siRNA delivery, such as its toxicity,[8] its ineffectiveness in certain types of cells,[9] and its potential of unwanted responses including its effects on autophagy in transfected cells.[10,11] Consequently, there are currently many studies focused on the design and development of carriers for siRNA delivery.[12−15] One of the nonviral based approaches is to use cell penetrating peptides (CPPs).[5,16]

CPPs are short strands of arginine- and/or lysine-rich peptides (<30 amino acids) that rely on their cationic nature for efficient intracellular accumulation. The conjugation of CPPs to drug molecules had been demonstrated to increase their cell uptake and biological effect.[17,18] CPPs have also been used for siRNA delivery by forming polyplexes, where the cationic CPPs can form noncovalent interactions with anionic siRNA.[19,20] However, the masking of cationic charges on CPPs has been shown to inhibit their uptake.[21] Therefore, studies using cationic or amphipathic CPPs for siRNA delivery might not fully take advantage of the peptides' delivery properties because the electrostatic interactions between CPP and siRNA

**Received:** September 20, 2011
**Revised:** December 9, 2011
**Accepted:** December 15, 2011
**Published:** December 15, 2011

  

could potentially diminish the CPP internalization capabilities. In this report, a unique polyplex, consisting of a chemically modified 21mer oligolysine peptide and siRNA, was designed to compare cationic, i.e. oligoarginine (R6), and amphipathic, i.e. model amphipathic peptide (MAP), CPPs for siRNA delivery. The ability of R6− and MAP−polyplexes to accumulate intracellularly and promote gene silencing activity via CPP-mediated delivery was also evaluated.

## EXPERIMENTAL SECTION

**Peptides and siRNA.** 21mer oligo-L-lysine (K21, KKKKKKKKKKKKKKKKKKKKK), $N_\alpha$-acetyl-tetra-L-arginine (Ac-R4, Ac-RRRR), $N_\alpha$-acetyl-hexa-L-arginine (Ac-R6, Ac-RRRRRR), $N_\alpha$-acetyl-octa-L-arginine (Ac-R8, Ac-RRRRRRRR), $N_\alpha$-L-cysteinyl model amphipathic peptide (CMAP, CKLALKLALKALKAALKLA) and $N_\alpha$-L-cysteinyl-hexa-L-arginine (CR6, CRRRRRR) were synthesized by Genemed Synthesis, Inc. (San Antonio, TX). Green fluorescent protein (GFP)-targeting siRNA (siGFP, sense, 5′-CAAGCUGACCCUGAAGUUdTdT-3′; antisense, 5′-GAACUUCAGGGUCAGCUUdTdT-3′)[22] and fluorophore-labeled negative control siRNA (siDY547, sense, 5′-DY547-UUCUCCGAACGUGUCACGUdTdT-3′; antisense, 5′-ACGUGACACGUUCGGAGAAdTdT-3′)[23] were obtained from Dharmacon (Lafayette, CO). Unlabeled negative control siRNA (siNC) and phosphatase and tensin homologue deleted on chromosome 10 (PTEN)-targeting siRNA (siPTEN) were purchased from Ambion (Foster City, CA) and Cell Signaling Technology (Danvers, MA), respectively.

**Pyridyldithiol Modification of Oligolysine.** K21 was reacted with *N*-succinimidyl-3-(2-pyridyldithio) propionate (SPDP, Pierce, Rockford, IL) for 30 min at room temperature, and then the pyridyldithiol (PDP)-activated peptide product (K21-PDP) was purified using Sephadex G-25 (GE Healthcare, Uppsala, Sweden) size exclusion chromatography with PBS as the mobile phase (1 × 25 cm column dimensions). K21-PDP was detected by measuring absorbance at 220 nm using a UV spectrophotometer (Shimadzu, Columbia, MD). K21-PDP was then collected and filtered through a 0.2 $\mu$m polyethersulfone membrane (VWR, San Dimas, CA). 2,4,6-Trinitrobenzene sulfonic acid (TNBSA, Sigma-Aldrich, St. Louis, MO) was used, according to the manufacturer's instructions, to quantify the amino groups of K21-PDP. In brief, TNBSA was reacted with K21-PDP, and after 2 h incubation at 37 °C, the product's absorbance was detected at 335 nm. $N_\alpha$-Acetyl-L-lysine methyl ester HCl (Sigma-Aldrich) was used to produce a standard curve to quantify the concentration of free amines.[24] The degree of PDP modification on K21 was determined by reacting K21-PDP with dithiothreitol (DTT) for 30 min at room temperature. Reducing K21-PDP released pyridine-2-thione, whose absorbance can be measured at 343 nm and used to quantify the degree of PDP modification (pyridine-2-thione $\varepsilon$ = 8080/M·cm). The average number of PDP modifications per K21-PDP was 4-to-1.

**Agarose Gel Shift Assay.** Different concentrations of K21-PDP were mixed together with siGFP to form polyplexes at different amine-to-phosphate (N/P) ratios. In this article, the N/P value listed before a polyplex will indicate the N/P mixing ratio in which the polyplex was prepared (i.e. 2:1 N/P polyplex was prepared by mixing K21-PDP and siGFP at a 2:1 N/P ratio). After 30 min incubation at room temperature, the different N/P polyplexes were loaded onto a 2% agarose gel (containing ethidium bromide) and run for 30 min at 125 V.[6] Images of gel were taken using ChemiDoc XRS System (Bio-Rad, Hercules, CA). Furthermore, various conditions were applied, and then the samples were examined on a 2% agarose gel. Polyplexes prepared at different N/P ratios were incubated with trypsin (0.1 mg/mL) for 15 min at 37 °C, and 2:1 N/P polyplex were serially diluted in PBS. Additional treatments included using DTT treatment (200 mM) for 20 min at room temperature followed by trypsin treatment as described. Undiluted and 10-fold diluted R6− and MAP−polyplexes were also evaluated.

**Determination of N/P Interaction.** K21-PDP was mixed with siGFP at 2:1 N/P for 30 min at room temperature. K21-PDP, siRNA (each at the same concentrations as 2:1 N/P polyplex mixture), and 2:1 N/P polyplex were each reacted with TNBSA as previously described, and the resulting absorbance was detected at 335 nm. The difference of absorbance values between K21-PDP and polyplex represented the concentration of amines interacting with the phosphates of siRNA.

**Displacement Assay of K21-PDP by Oligoarginine CPPs in K21-PDP−siRNA Polyplexes.** The guanidine groups of Ac-R4, Ac-R6 and Ac-R8 were quantified using 9,10-phenanthrenequinone (PQ) (Sigma-Aldrich).[25] After mixing the peptides with PQ, the reaction was initiated with the addition of 2 N NaOH, and the samples were incubated for 1 h at 60 °C. 1.2 N HCl was then added to stop the reaction, and the fluorescence was measured at excitation 312 nm and emission 395 nm using a fluorescence spectrophotometer (Hitachi, Tokyo, Japan). $N_\alpha$-Acetyl-L-arginine (Sigma-Aldrich) was used to produce a standard curve to quantify the guanidine groups. After quantifying the acetylated-peptides, 2:1 N/P polyplexes were incubated with different oligoarginine lengths (Ac-$R_n$, $n$ = 4, 6, 8) at different guanidine-to-amine (G/N) ratios (0.3:1, 1:1, 3:1) for 24 h at room temperature. TNBSA assay was performed to measure the presence of free K21-PDP amines. The difference between absorbance values of 2:1 N/P polyplex alone and 2:1 N/P polyplex mixed with oligoarginine peptides indicated the amount of K21-PDP amines in the polyplex displaced by the guanidines of oligoarginine.

**Preparation of R6−Polyplex and MAP−Polyplex.** K21-PDP was mixed with siRNA at 2:1 N/P for 30 min at room temperature. CR6 and CMAP were dissolved in sodium acetate buffer (pH 4.5) and added to the polyplex at a 1:1 CPP/PDP ratio (unless specified otherwise). CR6 and CMAP were synthesized with a cysteine group at the N-terminus, so that the thiol group could react with K21-PDP for conjugation. The reaction proceeded overnight at room temperature to generate the products, R6−polyplex and MAP−polyplex. Reaction efficiency for each product was determined by measuring absorbance at 343 nm.[26] The final stock concentrations of K21-PDP, siRNA and carrier CPP were 12.5, 2.5, and 60 $\mu$M, respectively. In this article, the polyplex nomenclature will include the carrier name followed by the type of siRNA used in the polyplex (i.e. MAP−polyplex with siGFP will be designated as "MAP−siGFP-polyplex"). In addition, any delivery vehicle carrying siRNA will be defined by the siRNA concentration.

Additional groups were also prepared. MAP−polyplex was also prepared at a lower CPP/PDP ratio (0.5:1 CPP:PDP MAP−siRNA polyplex) with a final carrier CPP concentration of 30 $\mu$M. A complex consisting of R6 or MAP and siRNA alone (R6/siRNA and MAP/siRNA) (i.e. without K21-PDP) was also prepared by mixing the two together at 60 and 2.5 $\mu$M, respectively, for 20 min at room temperature.

**Scheme 1. Development of Hexa-L-arginine (R6)−Polyplex and Model Amphipathic Peptide (MAP)−Polyplex for Comparison of Cationic and Amphipathic Cell Penetrating Peptides (CPPs) for siRNA Delivery and Efficacy[a]**

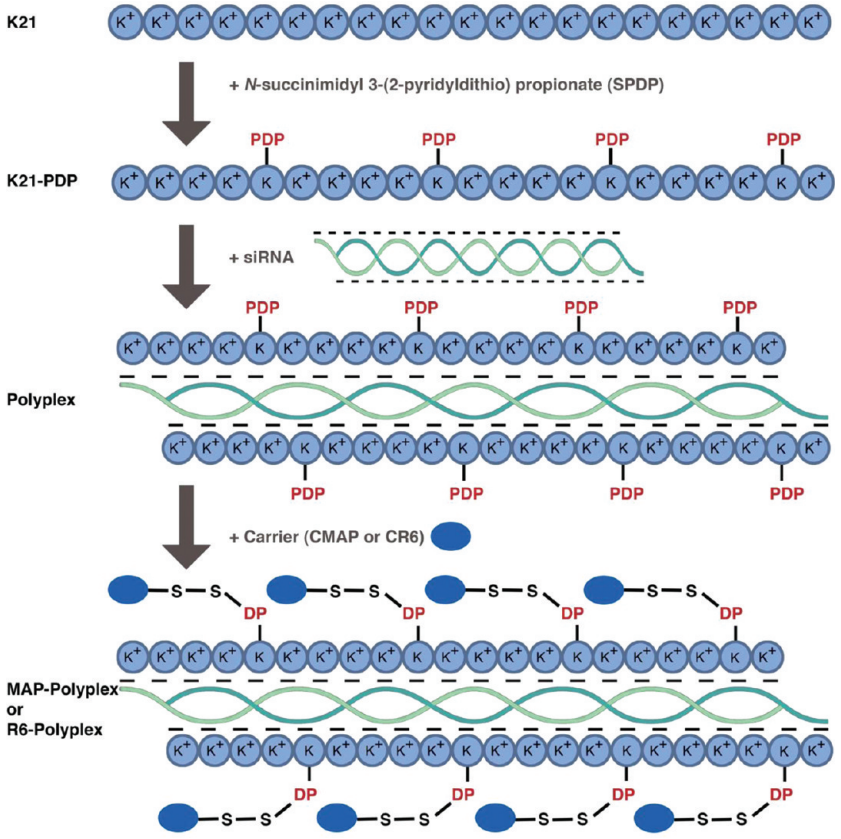


[a]Oligolysine (K21) was reacted with *N*-succinimidyl 3-(2-pyridyldithio) propionate to form the pyridyldithiol (PDP)-activated K21 (K21-PDP). The chemically modified product was purified using size exclusion chromatography, and the degree of modification was determined to be an average of 4 PDP per K21-PDP. K21-PDP was mixed with siRNA for 30 min at room temperature to form a polyplex, and then R6 or MAP was added to the polyplex solution to produce R6−polyplex or MAP−polyplex, respectively. The reaction proceeded overnight, and the carrier CPP was conjugated to the polyplex via a reducible disulfide bond. The conjugate products were then ready for evaluation.

**Cytotoxicity Assay.** Huh7.5 cells, stably transfected to express GFP-light chain 3 protein (GFP-LC3), were used for evaluation of R6−polyplex and MAP−polyplex. The characterization of these cells, transfected with pGFP-LC3 followed by G418 (Invitrogen, Carlsbad, CA) selection, was previously described.[27] Cells were maintained at 37 °C, 5% $CO_2$ in Dulbecco's modified Eagle's medium (DMEM) supplemented with 10% fetal bovine serum (FBS), 1% nonessential amino acids, and 2 mM L-glutamine ("Huh7.5 complete medium") (Invitrogen). As a positive control, Lipofectamine 2000 (Invitrogen) was used to deliver siRNA according to manufacturer's instructions. In brief, immediately prior to transient transfection, Lipofectamine 2000 was mixed with siRNA in serum-free medium, OptiMEM (Invitrogen), at the recommended ratio of 1 $\mu$L of Lipofectamine 2000 per 20 pmol of siRNA. Treated Huh7.5 cells were evaluated for cell viability at 48 h from the start of treatment using 3-(4,5-dimethylthiazol-2-yl)-2,5-diphenyltetrazolium bromide (MTT) (Sigma-Aldrich).[28] MTT solution was added to the Huh7.5 complete medium and incubated for an additional 4 h. Medium was then removed from the cells and replaced with 1:24 1 N HCl:isopropanol solution. Once the cells were thoroughly dissolved, cell viability was measured using a plate reader (Tecan, Männedorf, Switzerland) at a wavelength of 570 nm.

**Cellular Uptake Assay.** SiDY547 was used for cell uptake assays in Huh7.5 cells. Cells were treated with the dosing solutions prepared in OptiMEM for 1 and 6 h at 37 °C, 5% $CO_2$. At the designated time points, the cells were washed with 4 °C PBS, trypsinized and lysed with cell extraction buffer (Invitrogen) supplemented with protease inhibitor cocktail and phenylmethylsulfonyl fluoride (Sigma-Aldrich). The cell lysates were transferred to a 96-well plate for fluorescence detection of siDY547 using a microplate reader (Molecular Devices, Sunnyvale, CA) with excitation at 544 nm and emission at 590 nm. Thereafter, cell lysates were quantified for protein content using bicinchoninic acid (BCA) Assay (Pierce). SiDY547 fluorescence was defined as relative fluorescence units (RFU) per mg of cell protein.

Temperature-based cell uptake assays were conducted similarly. Transferrin (Sigma-Aldrich) was labeled with $Na^{125}I$ ($^{125}I$-Tf) (PerkinElmer, Inc., Waltham, MA) using the Chloramine-T method.[29] 50 nM MAP−siDY547-polyplex was coincubated with 3 $\mu$g/mL $^{125}I$-Tf in OptiMEM for 1 h treatment of Huh7.5 cells at 4, 16, and 37 °C. Analysis of siDY547 was performed as previously described, whereas $^{125}I$-Tf in the cell lysate was detected using a gamma counter (Packard, Downers Grove, IL).

**Gene Silencing Effect Assays.** SiGFP was used to silence the fluorescence produced by GFP-LC3 expressed in Huh7.5


dx.doi.org/10.1021/mp200481g | *Mol. Pharmaceutics* 2012, 9, 299−309

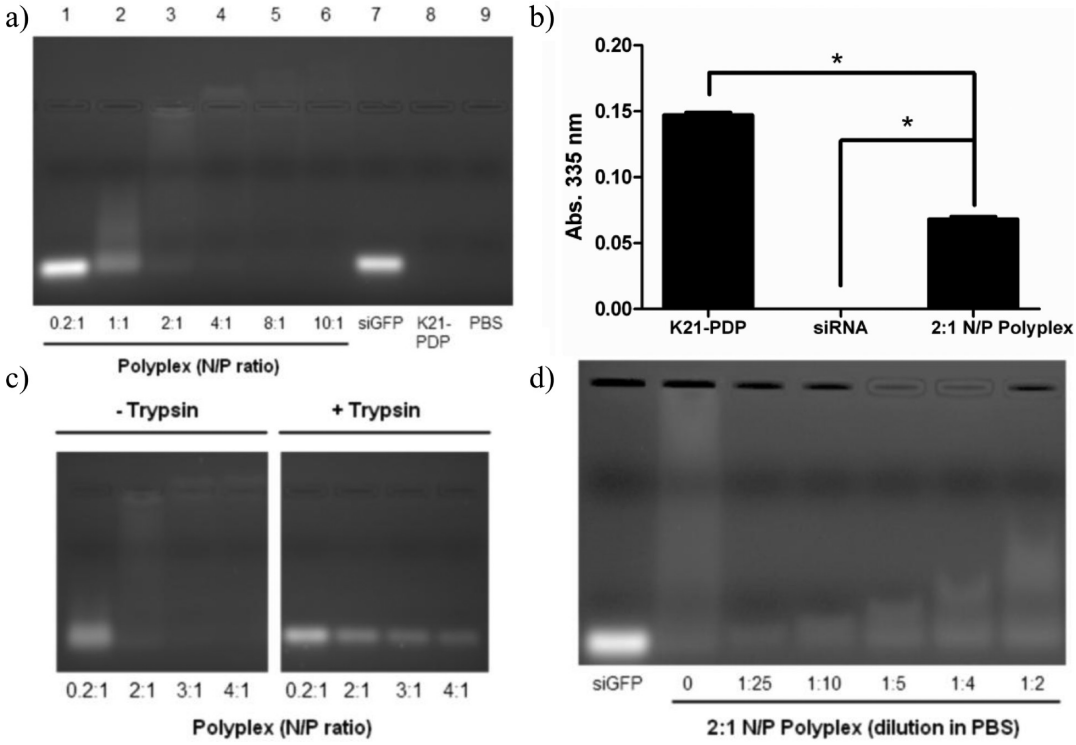


**Figure 1.** Polyplex formation and dissociation. (a) K21-PDP and siGFP were mixed together for 30 min at room temperature at different N/P ratios to form polyplexes. Different N/P polyplexes were loaded on a 2% agarose gel containing ethidium bromide and run at 125 V for 30 min. (b) Determination of N/P interaction for 2:1 N/P polyplex. TNBSA was reacted with 2:1 N/P polyplex and then samples were detected at a wavelength of 335 nm. Error bars represent standard deviation ($n = 3$). Asterisk (*) indicates $p < 0.05$ based on analysis of variance and the Bonferroni test. (c) siRNA release from different N/P polyplexes after trypsin digestion. (d) siRNA release after dilution of 2:1 N/P polyplex in PBS.

cells.[11] Cells were transiently transfected for 6 h in OptiMEM, and then the treatments were replaced with Huh7.5 complete medium for additional 42 h incubation. The cell lysates were collected as previously described and transferred to a 96-well plate for fluorescence detection of GFP-LC3 using a microplate reader (Tecan) with excitation at 485 nm and emission at 518 nm. The protein content of the cell lysates was determined using BCA assay. GFP-LC3 fluorescence was defined as RFU per mg of cell protein. siNC-loaded delivery vehicles were used to compare the relative silencing efficiencies by siGFP-loaded counterparts. To evaluate the transfection efficiency in the presence of 10% FBS, treatments were conducted similarly as described, except that cells were transiently transfected for 6 h in Huh7.5 complete medium.

SiPTEN was used to silence PTEN gene expression in HeLa cells (ATCC, Manassas, VA). HeLa cells were maintained at 37 °C, 5% $CO_2$ in DMEM supplemented with 10% FBS and 2 mM L-glutamine ("HeLa complete medium") (Invitrogen). Cells were transiently transfected for 6 h in OptiMEM with 100 nM siPTEN (based on manufacturer's recommendations) using Lipofectamine 2000 complexes and MAP−polyplexes, and then the treatments were replaced with HeLa complete medium for an additional 42 h incubation. After protein quantification of cell lysates using BCA assay, equal amounts of cellular protein (40 $\mu$g) were subjected to electrophoresis in 13% SDS−PAGE gels followed by Western blotting using anti-PTEN (Cell Signaling Technologies) and anti-$\beta$-actin (Sigma-Aldrich) primary antibodies with corresponding secondary HRP-conjugated secondary antibodies (Sigma-Aldrich). Immunoreactive bands were detected using enhanced chemiluminescence (GE Healthcare) and quantified using Quantity One (Bio-Rad, Hercules, CA).

**Statistical Analysis.** Data were presented as mean with error bars representing standard deviation and analyzed by analysis of variance and the Bonferroni multiple comparison test. Results designated with an asterisk (*) were statistically significantly different ($p < 0.05$).

## RESULTS

**Design of Oligolysine Polyplex.** The procedure for the preparation of the CPP-conjugated siRNA polyplexes is illustrated in Scheme 1. There were two important considerations for the K21-PDP−siRNA polyplex design. siRNA must be stably bound to oligolysine to form the polyplex, but once internalized, it has to be released from the polyplex to produce a gene silencing effect. K21-PDP and siGFP were mixed together at different N/P ratios, and the formation of polyplex was observed using a gel shift assay.[6] It was found that mixing K21-PDP and siGFP at a 2:1 N/P ratio was optimal for polyplex formation (Figure 1a, lane 3) because it was the minimal N/P ratio where no free siRNA was detected compared with uncomplexed siRNA (Figure 1a, lane 7). In addition, a band shift was observed to indicate that the siRNA was neutralized and had formed a polyplex.[30] TNBSA assay was performed to calculate the actual N/P interaction between the K21-PDP amine groups and siRNA phosphate groups. When K21-PDP and siGFP were mixed together at 2:1 N/P, there was a loss of absorbance, which was calculated as a ~1:1 N/P interaction (Figure 1b). The electrostatic interaction between the amine and phosphate groups prevented TNBSA reaction with the lysine amines, which reduced the signal at a

wavelength of 335 nm.[31] The siRNA bound in a polyplex could also be released from the structure by two methods. First, polyplexes were prepared at different N/P ratios (0.2–4:1 N/P), and then the degradation of K21-PDP after treatment with trypsin was evaluated by agarose gel shift assays. As shown in Figure 1c, regardless of the mixing N/P ratio of the polyplex, free siRNA was detected after incubation with trypsin. On the other hand, siRNA could also be released by diluting the polyplex. As the polyplex was diluted to lower concentrations (1:2 to 1:25 dilution), its stability was weakened, and siRNA was detectable at a position corresponding to free siRNA (Figure 1d).

**Selection of Oligoarginine Peptide Length.** Oligoarginine was considered for conjugation to the polyplex because it has been shown to localize in the cytosol following internalization.[32] Cytosolic localization was preferable since RNAi occurs in this compartment.[13] The length of the cationic CPP is an important factor in its delivery efficiency.[33] However, for the design of our polyplex, there were concerns that oligoarginine could displace K21-PDP's interaction with siRNA since the guanidine group of arginine is a stronger base than the $\varepsilon$-amine group of lysine. Therefore, different lengths of oligoarginine—Ac-R4, Ac-R6, and Ac-R8—were incubated with 2:1 N/P polyplex at different G/N ratios to evaluate whether any displacement would occur. Displacement of K21-PDP was detected using TNBSA assay due to an increased signal detected at 335 nm with each unbound lysyl-amine group. The $\alpha$-amine groups of the oligoarginine peptides were N-acetylated so that they would not react with TNBSA. As shown in Figure

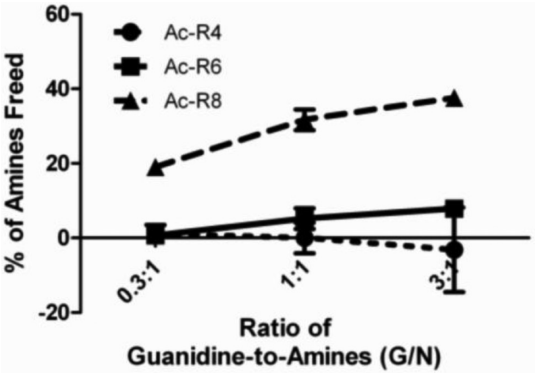


**Figure 2.** Selection of oligoarginine length for conjugation to polyplex. Ac-R4, Ac-R6 and Ac-R8 were incubated with 2:1 N/P polyplex at different G/N ratios for 24 h. TNBSA was reacted with the samples, and then absorbance at a wavelength of 335 nm was measured. Data are presented as a percentage of amines released compared with 2:1 N/P polyplex.

2, no significant displacement was observed between 0.3:1, 1:1 and 3:1 G/N when incubating 2:1 N/P polyplex with Ac-R4 (1, 0, −3% displacement, respectively, $p > 0.05$) or Ac-R6 (0.7, 5, 8%, respectively, $p > 0.05$). However, Ac-R8 exhibited significantly greater displacement of the polyplex at 1:1 G/N (32%, $p < 0.01$) and 3:1 G/N (38%, $p < 0.001$) vs 0.3:1 G/N (19%). Furthermore, Ac-R8 significantly displaced more K21-PDP than Ac-R6 and Ac-R4 at all three G/N ratios ($p < 0.001$), whereas Ac-R6 only showed significant differences compared to Ac-R4 at 3:1 G/N ($p < 0.05$). These results indicated that peptide length and G/N ratio had significant effects on polyplex stability. Based on these results, R6 was selected to conjugate to polyplex because it was the longest arginine CPP with minimal polyplex displacement (<10%).

**Stability of CPP–Polyplex.** The stability of MAP– and R6–polyplex was evaluated by conducting an agarose gel shift assay. MAP– and R6–polyplex did not exhibit any signal because ethidium bromide was unable to access and intercalate with the loaded siRNA (Figure 3, lanes 3, 4). Upon 10-fold

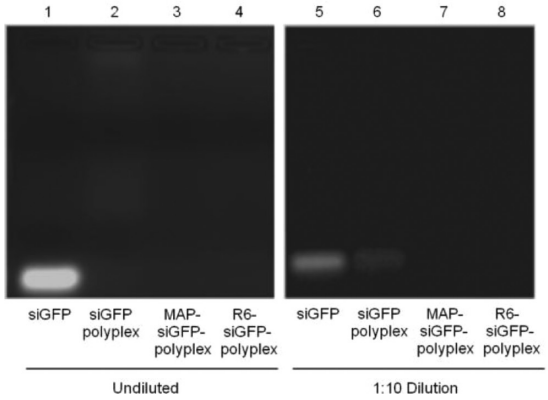


**Figure 3.** CPP–polyplex stability. To demonstrate CPP–polyplex stability, undiluted and 10-fold diluted (in PBS) siGFP, 2:1 N/P siGFP polyplex, MAP–polyplex and R6–polyplex were loaded on a 2% agarose gel containing ethidium bromide and run at 125 V for 30 min.

dilution in PBS, MAP– and R6–polyplex did not release any detectable siRNA (lanes 7, 8), whereas 10-fold diluted polyplex showed free siRNA (lane 6).

**Cell Viability.** A potential side effect of CPPs was their cytotoxicity to the cells. MTT assay was used to determine the cell viability of Huh7.5 cells after treatment. Although polyplex, R6–polyplex and MAP–polyplex reduced cell viability by 5, 6 and 17%, respectively, compared with nontreated cells, none of these changes were found to be significant (Figure 4). In addition, these reductions were similar to the cytotoxic effect

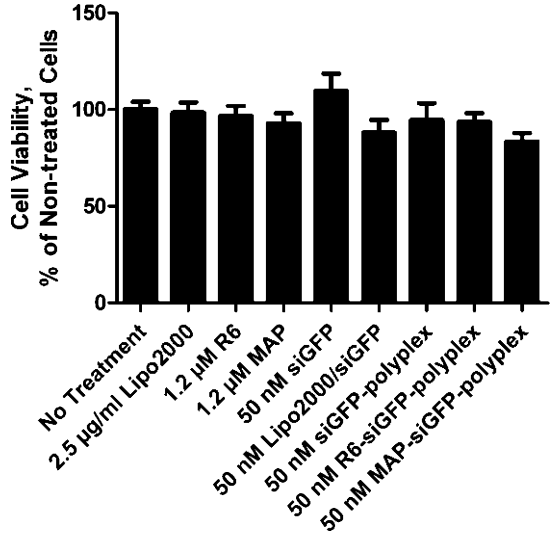


**Figure 4.** Cell viability. Stably transfected Huh7.5 cells were treated for 6 h in OptiMEM before being replaced with Huh7.5 complete medium for an additional 42 h. MTT solution was added to the completed medium for an additional 4 h treatment. Then, the cells were dissolved in 1:24 1 N HCl:isopropanol solution, and cell viability was measured at a wavelength of 570 nm.

observed for Lipofectamine 2000 complexes (12%) (Figure 4). Therefore, treatments with 50 nM R6−polyplex and MAP−polyplex were not significantly cytotoxic, and cell viability was maintained.

**Cellular Uptake of R6−Polyplex and MAP−Polyplex.** SiDY547, a fluorophore labeled negative control siRNA, was used to compare the intracellular delivery efficiency of cationic R6 and amphipathic MAP in Huh7.5 cells. DY547-siRNA was combined with K21-PDP to form a 2:1 N/P polyplex (siDY547-polyplex). Subsequently, each CPP was conjugated to the polyplexes via a reducible disulfide bond to form R6−siDY547-polyplex and MAP−siDY547-polyplex. MAP−siDY547-polyplex (50 nM) exhibited 4- and 3-fold greater cellular uptake of siDY547 than 50 nM Lipofectamine 2000 complex at 1 and 6 h, respectively (Figure 5). On the other hand, 50 nM siDY547, siDY547-polyplex and R6−siDY547-polyplex demonstrated minimal uptake at both time points (Figure 5). Each CPP was also treated with the cells alone to demonstrate that neither emitted fluorescence at that excitation wavelength (Figure 5).

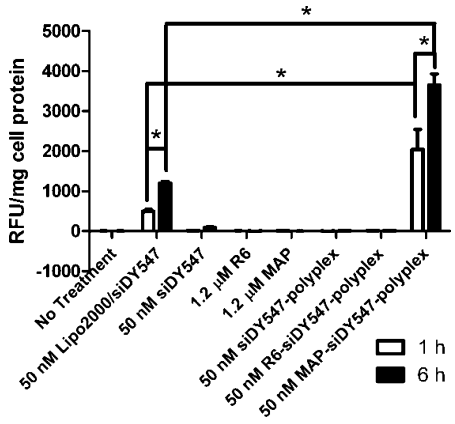


**Figure 5.** Cellular uptake. To measure the siRNA uptake, Huh7.5 cells, stably transfected to express GFP-LC3, were treated for 1 and 6 h in OptiMEM. After treatment, cells were washed and lysates were collected. Cell lysates were measured at Ex. 544 and Em. 590 nm and normalized with protein concentrations quantified using BCA assay. Error bars represent standard deviation ($n$ = 3). Asterisk (*) indicates $p < 0.05$ based on analysis of variance and the Bonferroni test.

**Gene Silencing Effects by R6−Polyplex and MAP−Polyplex.** Huh7.5 cells, stably transfected to express GFP-LC3 fusion protein, were used to evaluate the gene silencing efficacy by R6−polyplex and MAP−polyplex. R6−polyplexes and MAP−polyplexes were loaded with siRNA targeting GFP of the fusion protein (R6−siGFP-polyplex and MAP−siGFP-polyplex), while a nontargeting negative control siRNA was used for control groups (R6−siNC-polyplex and MAP−siNC-polyplex). Compared with the siNC-loaded counterpart, MAP−siGFP-polyplex (50 nM) demonstrated a 53% reduction in fluorescence signal, while siGFP- and R6−siGFP-polyplexes (50 nM) exhibited an insignificant silencing of 9 and 0%, respectively (Figure 6a). In addition, 50 nM MAP−siGFP-polyplex exhibited a comparable fluorescence knockdown with 50 nM Lipofectamine 2000/siGFP complex (53 ± 6.1% vs 60 ± 6.8%, respectively, Figure 6a).

**Role of K21-PDP for CPP−Polyplex Activity.** A complex made only of R6 or MAP and siGFP (R6/siGFP and MAP/siGFP) was prepared to demonstrate the disadvantage of not first neutralizing siRNA with K21-PDP and then conjugating the carrier peptide to the polyplex. Treatment with 50 nM R6/siGFP, R6−siGFP-polyplex or MAP/siGFP did not exhibit any significant silencing effect compared with 50 nM siGFP (Figure 6b). However, there was a significant difference in fluorescence knockdown between 50 nM MAP/siGFP (without K21-PDP) and MAP−siGFP-polyplex (with K21-PDP) (Figure 6b).

**Evaluation of MAP−Polyplex Activity in the Presence of Serum.** The effect of serum on MAP−polyplex activity was evaluated by comparing OptiMEM (serum-free) with Huh7.5 complete medium (containing 10% FBS) for transfection. MAP−siGFP-polyplex (50 nM) produced a GFP fluorescence knockdown of 49 and 47% when Huh7.5 cells were transiently transfected in OptiMEM and Huh7.5 complete medium, respectively (Figure 6c). On the other hand, 50 nM siGFP did not reduce fluorescence at 48 h in either medium. Therefore, MAP−siGFP-polyplex activity exhibited comparable silencing effects in OptiMEM and Huh7.5 complete medium.

**Gene Silencing Effect of MAP−Polyplex on an Endogenous Gene.** MAP−polyplex efficacy was further evaluated by targeting endogenous gene expression (PTEN) in an alternative cell line (HeLa). PTEN is a lipid phosphatase that negatively mediates the mitogenic signaling phosphoinositide 3-kinase (PI3K)/AKT signaling pathway, and loss of PTEN function promotes growth and survival phenotypes.[34,35] HeLa cells were treated with 100 nM siPTEN using Lipofectamine 2000 complexes and MAP−polyplexes and then evaluated for PTEN expression using Western blotting. MAP−siPTEN-polyplex reduced PTEN protein levels by ∼50%, whereas siPTEN alone did not exhibit any significant gene silencing effect (Figure 6d). Furthermore, 100 nM MAP−siPTEN-polyplex exhibited efficacy comparable to that of 100 nM Lipofectamine 2000/siPTEN complex.

**Role of MAP for MAP−Polyplex Delivery and Activity.** The importance of the MAP:polyplex ratio on internalization and activity was evaluated by comparing the amphipathic CPP polyplex at different ratios of MAP to PDP groups. MAP−siDY547-polyplex (50 nM) formed at 1:1 CPP:PDP produced a significant 60% increase of uptake compared with 0.5:1 CPP:PDP MAP−siDY547-polyplex (Figure 7a). Correspondingly, the activity exhibited by MAP−siGFP-polyplex was dose-dependent on MAP:polyplex ratio, where the 0.5:1 and 1:1 CPP:PDP MAP−siGFP-polyplex (50 nM) produced a fluorescence knockdown of 17 and 50%, respectively (Figure 7b). Coincubation of unconjugated MAP and DY547-polyplex at the same concentration as the 1:1 CPP:PDP polyplex showed minimal uptake, similar to the uptake of siDY547-polyplex (Figure 7a), and low fluorescence knockdown of 11% (Figure 7b). The silencing effect of siGFP-polyplex without MAP was insignificant (Figure 7b).

**Transport Mechanism of MAP−Polyplex.** MAP−polyplex demonstrated greater potential for siRNA delivery than R6−polyplex (Figures 5, 6a). Thus, further studies were conducted to investigate the cell entry properties of MAP−polyplex. MAP−siDY547-polyplex (50 nM) was coincubated with 3 μg/mL of radiolabeled $^{125}$I-Tf for cellular uptake assays at different temperatures (4, 16, and 37 °C). Endocytosis and intracellular vesicular fusion events were inhibited at 4 and 16 °C, respectively.[32] $^{125}$I-Tf, which enters cells through clathrin-mediated endocytosis,[36] was used as an internal standard and verified the loss of vesicle formation and fusion in Huh7.5 cells due to a 70 and 54% reduction of uptake at 4 and 16 °C, respectively (Figure 8a). More importantly, MAP−siDY547-

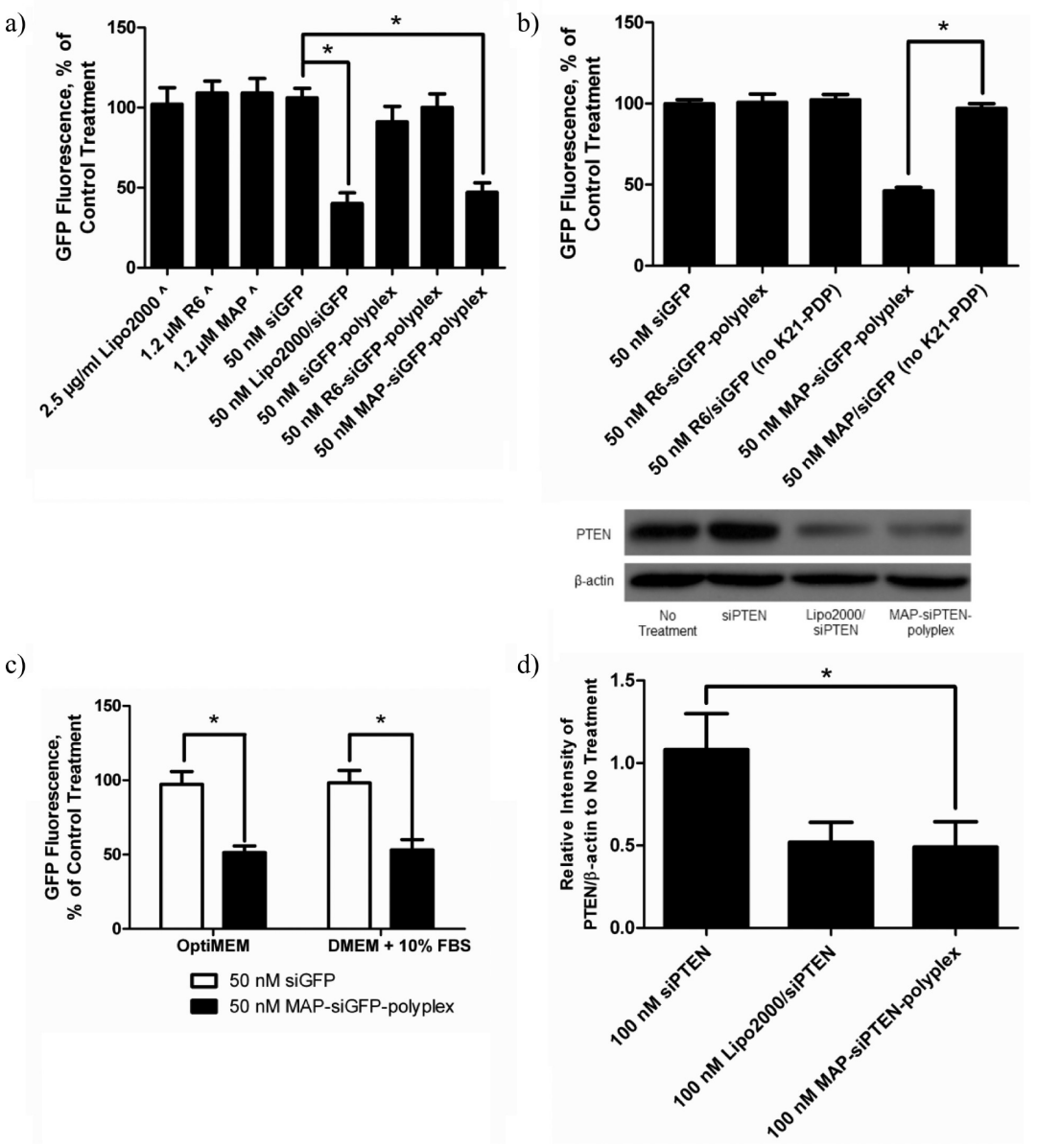


**Figure 6.** Gene silencing effects. (a, b, c) To measure GFP silencing effect, the stably transfected Huh7.5 cells were treated for 6 h in (a, b, c) OptiMEM (serum-free) or (c) Huh7.5 complete medium (containing 10% FBS) before being replaced with Huh7.5 complete medium for an additional 42 h. Cells were then washed, and lysates were collected. Cell lysates were measured at Ex. 485 nm and Em. 518 nm and normalized with protein concentrations quantified using BCA assay. (a) Data marked with a caret (∧) indicate the value is relative to no treatment; the other unmarked data are relative to siNC equivalent counterpart. (b) R6/siRNA and MAP/siRNA were prepared at the same concentrations as R6− and MAP−polyplex, with the exception of no K21-PDP. (d) To measure PTEN silencing effect, HeLa cells were treated for 6 h in OptiMEM before being replaced with HeLa complete medium for an additional 42 h. Cell lysates were collected, quantified using BCA assay, run on 13% SDS−PAGE and immunoblotted with anti-PTEN and anti-$\beta$-actin. Signal intensities were quantified using densitometry, and data was expressed as the average of relative intensities to nontreated cells. Error bars represent standard deviation ($n$ = 3). Asterisk (*) indicates $p < 0.05$ based on analysis of variance and the Bonferroni test.

polyplex also experienced a 52 and 35% reduction in uptake at 4 and 16 °C, respectively (Figure 8a).

**In Vitro Demonstration of siRNA Release from MAP−Polyplex.** MAP−polyplex was incubated with the reducing agent DTT and/or the enzyme trypsin to model the release of siRNA from MAP−polyplex. MAP−polyplex did not exhibit a signal when run on an agarose gel (Figure 8b, lane 6). However, after using DTT to reduce the disulfide bonds of MAP−polyplex, a pattern emerged that was similar to that of the polyplex (lane 7 vs lane 4). Trypsin treatment of reduced MAP−polyplex released siRNA from the polyplex (lane 8 vs lane 1) and was similar to polyplex treated directly with trypsin (lane 8 vs lane 5). However, treating MAP−polyplex with trypsin alone did not release free siRNA (lane 9 vs lane 1).

## DISCUSSION

CPPs have been previously studied for siRNA delivery applications.[5,16,19] However, the cationic or amphipathic CPPs typically used are directly complexed to the siRNA, which results in the neutralization of the CPP cationic charges. The loss of cationic/amphipathic properties of the CPP compromises its internalization efficiency. In this study, we


dx.doi.org/10.1021/mp200481g | Mol. Pharmaceutics 2012, 9, 299−309

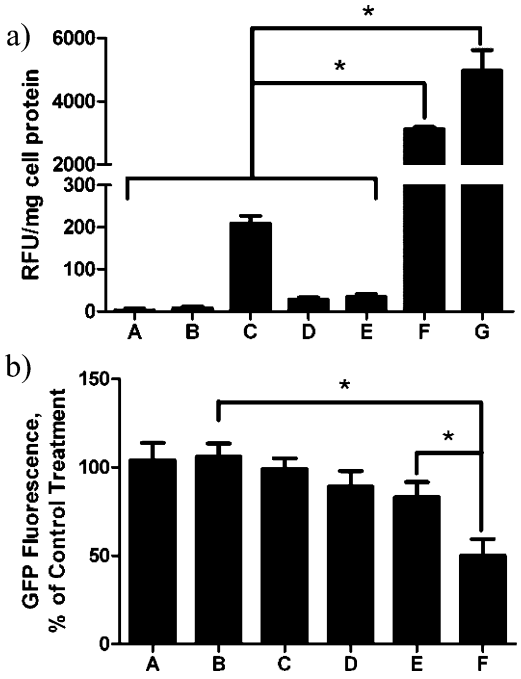


**Figure 7.** Comparison of different amounts of MAP conjugation for MAP−polyplex cellular uptake and GFP silencing effect. MAP−polyplexes were prepared with different amounts of MAP conjugation. (a) To measure siRNA uptake, stably transfected Huh7.5 cells were treated for 6 h in OptiMEM. After treatment, cells were washed and lysates were collected. Cell lysates were measured at Ex. 544 and Em. 590 nm and normalized with protein concentrations quantified using BCA assay: A, no treatment; B, 1.2 $\mu$M MAP; C, 50 nM siDY547; D, 50 nM siDY547-polyplex; E, 50 nM siDY547-polyplex + 1.2 $\mu$M MAP; F, 50 nM 0.5:1 CPP/PDP MAP−siDY547-polyplex; G, 50 nM 1:1 CPP/PDP MAP−siDY547-polyplex. (b) To measure GFP silencing, after a 6 h transfection and an additional incubation with Huh7.5 complete medium for 42 h, cells were washed and lysates were collected. Cell lysates were measured at Ex. 485 nm and Em. 518 nm and normalized with protein concentrations quantified using BCA assay. Error bars represent standard deviation ($n$ = 3): A, 1.2 $\mu$M MAP; B, 50 nM siGFP; C, 50 nM siGFP-polyplex; D, 50 nM siGFP-polyplex +1.2 $\mu$M MAP (unconjugated); E, 50 nM 0.5:1 CPP/PDP MAP−siGFP-polyplex; F, 50 nM 1:1 CPP/PDP MAP−siGFP-polyplex. Data are presented relative control treatments (A, relative to nontreated cells; B−F, relative to siNC equivalent counterpart). Asterisk (*) indicates $p < 0.05$ based on analysis of variance and the Bonferroni test. Error bars represent standard deviation ($n$ = 3).

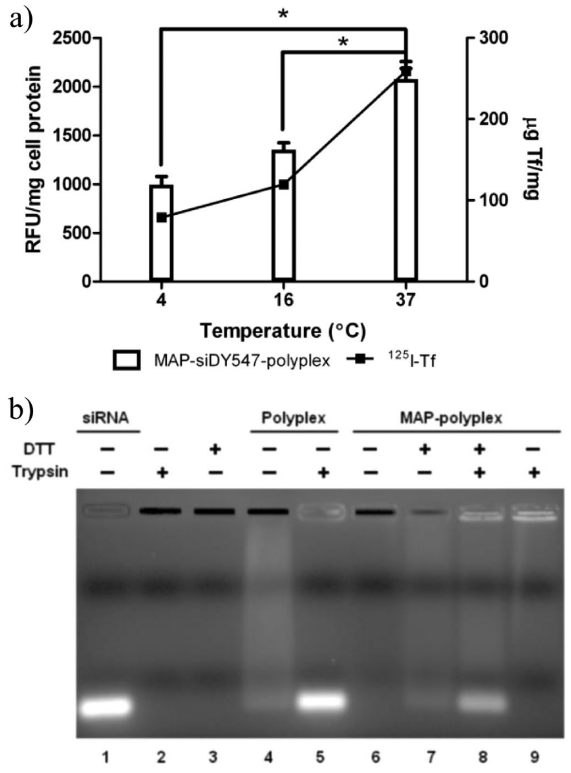


**Figure 8.** Transport Mechanism of MAP−polyplex and in vitro demonstration of siRNA release from MAP−polyplex. (a) Stably transfected Huh7.5 cells were treated with 50 nM MAP−siDY547-polyplex and 3 $\mu$g/mL $^{125}$I-Tf for 1 h in OptiMEM at 4, 16, and 37 °C. Cells were washed, and lysates were collected. Cell lysates were measured at Ex. 544 and Em. 590 nm for siDY547 uptake and using a gamma counter for $^{125}$I-Tf uptake. Error bars represent standard deviation ($n$ = 3). Asterisk (*) indicates $p < 0.05$ based on analysis of variance and the Bonferroni test. (b) 2:1 N/P polyplex and MAP−polyplex were incubated with DTT and/or trypsin and loaded on a 2% agarose gel running at 125 V for 30 min. Lane 1: siRNA. Lane 2: trypsin. Lane 3: DTT. Lane 4: 2:1 N/P polyplex. Lane 5: 2:1 N/P polyplex + trypsin. Lane 6: MAP−polyplex. Lane 7: MAP−polyplex + DTT. Lane 8: MAP−polyplex + DTT + trypsin. Lane 9: MAP−polyplex + trypsin.

were able to avoid the CPP neutralization by designing a unique siRNA polyplex containing two CPP moieties that each served a specific function: a CPP for siRNA neutralization and a CPP for siRNA delivery. This design provided a direct comparison of the siRNA delivery capabilities by cationic and amphipathic CPPs.

With regard to using a cationic polymer to neutralize siRNA, the 21mer oligolysine K21 was chosen to form a polyplex with siRNA due to its following advantages. First, siRNA duplexes typically contain 21 base pairs in length.[37] K21 sequence was selected because the number of charges would provide a good match with the siRNA backbone and allowed strong electrostatic interaction between the two moieties. Second, K21 contained the $\varepsilon$-amino groups of the lysyl residues, which can be chemically modified to conjugate the polyplex to CPP delivery moieties. A heterobifunctional cross-linker, SPDP, was used to link the polyplex with carrier CPPs via a reducible disulfide bond linker to enable the separation of the carrier CPPs from the K21-PDP−siRNA polyplex after internalization into cells. Third, the potential digestion of K21 by cytosolic lysine-specific proteases could facilitate siRNA release from the polyplex.[38,39]

Whether K21-PDP functioned as a suitable neutralizing CPP was determined on the basis of its ability to sufficiently form a stable neutral polyplex and efficiently release siRNA from the polyplex after cellular uptake.[30] A mixture of 2:1 N/P ratio exhibited a fully neutralized complex because no free siRNA was detected (Figure 1a). The neutralization was confirmed by determining a ∼1:1 N/P interaction for polyplexes prepared at 2:1 N/P ratio (Figure 1b). Increasing the N/P ratio led to increased positive charges of the polyplexes since the band migrated above the loading well (Figure 1a, 4:1 to 10:1). On the other hand, the release of siRNA from the polyplex was verified either by trypsin treatment that digested K21-PDP in 0.2:1 to 4:1 N/P polyplex (Figure 1c) or by dilution effects that weakened the electrostatic interactions for 2:1 N/P polyplex (Figure 1d). Therefore, these data indicated that not only could


dx.doi.org/10.1021/mp200481g | Mol. Pharmaceutics 2012, 9, 299−309

K21-PDP form polyplexes with siRNA but it could also release the oligonucleotides under certain conditions.

Two different types of CPPs were compared for the delivery of this neutralized K21-PDP−siRNA polyplex. In this study, cationic (R6) and amphipathic (MAP) CPPs were compared and evaluated for siRNA delivery and efficacy. Cationic oligoarginine was considered because its cellular localization following internalization is mainly cytosolic, where RNAi originates. Several oligoarginine peptides were compared, and cationic R6 was selected because it was the longest oligoarginine peptide that did not significantly displace K21-PDP from the polyplex (Figure 2). On the other hand, previous studies from our lab reported that amphipathic MAP exhibited significantly greater cellular uptake than other CPPs, such as oligoarginine, but subcellular fractionation studies indicated that MAP was found primarily in the vesicular fraction and not detectable in the cytosolic portion.[40] Thus, the purpose of our comparison was to determine whether the intracellular localization or the amount of cellular uptake would be the most important factor for siRNA efficacy.

Our results suggested that MAP was a more suitable CPP for siRNA delivery than R6. Not only did MAP demonstrate significantly greater intracellular delivery of siDY547 (Figure 5), but it also produced a better knockdown of GFP fluorescence (Figure 6a). Temperature-based uptake assays showed that MAP−polyplex intracellular delivery required vesicle formation and fusion (Figure 8a), which was consistent with the proposed properties of MAP alone.[40] The observed silencing effect indicated that MAP−polyplex was capable of endosomal escape to deliver siRNA into the cytosol for gene silencing. It had been reported that amphipathic peptides exhibited endosomal escape properties.[41−43] It is plausible that MAP−polyplex shared such properties and was able to deliver the siRNA cargo into the cytosol. On the other hand, R6−polyplex was more limited in terms of uptake and silencing effects, where a lack of intracellular siDY547 was observed (Figure 5) and no GFP knockdown was detected (Figure 6a). These results were similar with those observed for siRNA polyplex without CPP conjugation (Figure 5, 6a). Thus, conjugated R6 was unable to facilitate polyplex delivery. Furthermore, R6/siRNA, without any K21-PDP, was also unable to produce a gene silencing effect at carrier and siRNA concentrations equivalent to R6−polyplex (Figure 6b). However, the oligoarginine CPP did exhibit less cytotoxicity than MAP, whether it was given free or as a CPP−polyplex, but this difference was not significant (Figure 4).

Both CPP−polyplexes exhibited similar conjugation efficiencies between the CPP carrier and polyplex (between 77 and 88% based on pyridine-2-thione absorbance at 343 nm). In addition, the conjugation of either CPP carrier stabilized the polyplex so that siRNA was not released after 10-fold dilution (Figure 3). The lack of siRNA release by CPP carrier conjugated to the polyplex may be attributed to steric stabilization.[44] Despite these similarities between the CPP−polyplexes, the cationic R6−polyplex was not as effective as the amphipathic MAP−polyplex for getting sufficient amounts of the polyplex into the cell to elicit a biological response. These observations were particularly interesting since MAP contains only one less cationic charge than R6 (5 vs 6, respectively). Thus, the number of cationic charges alone did not necessarily correlate to the delivery efficiency by a CPP. Instead, the distribution of cationic charges among hydrophobic regions in the amphipathic MAP demonstrated the importance of amino acid sequence for efficient cellular uptake and activity of siRNA polyplex. Another important factor could be the CPP size. MAP was 19 amino acids in length, whereas R6 was only 7 (including the cysteine at the N-terminus). The longer peptide may have had more accessibility to the extracellular surface in order to facilitate polyplex uptake.

Interestingly, MAP−polyplex delivered significantly greater amounts of siRNA than Lipofectamine 2000 complex (Figure 5), but only exhibited comparable levels of gene knockdown in Huh7.5 cells (Figure 6a). MAP had previously been reported to have nuclear localization and enter the cell through a vesicle-based process.[40] Thus, a large portion of the internalized siRNA may have been delivered to compartments, such as the nucleus or lysosome, where RNAi cannot be initiated. However, a fraction of MAP−polyplex must have escaped the vesicles and into the cytosol since gene silencing was observed. MAP−polyplexes and Lipofectamine 2000 complexes also exhibited comparable gene silencing effects in HeLa cells when targeting the endogenous gene, PTEN (Figure 6d). Mediating PTEN function had recently been proposed as a potential therapeutic approach for recovery from adult spinal cord injury.[45]

We proposed the mechanism of siRNA release in the cytosol after MAP−polyplex endosomal escape using an in vitro demonstration. MAP−polyplex was believed to have its disulfide bonds cleaved by the reducing environment of the cytosol,[46] which would expose the polyplex to cytosolic peptidases to free the siRNA. We demonstrated this proposed breakdown of MAP−polyplex by using DTT and trypsin treatment to simulate cytosolic reducing and peptidase activities, respectively. DTT separated the carrier and polyplex by reducing the disulfide bonds between MAP and polyplex, and subsequent trypsin treatment of the unconjugated polyplex cleaved the K21-PDP peptides and released siRNA (Figure 8b, lane 8). However, when MAP−polyplex was treated directly with trypsin, siRNA was not freed (Figure 8b, lane 9). The release of siRNA from the delivery vehicle was a pertinent consideration for the design of MAP−polyplex because if the siRNA remained bound in the polyplex, then it would be unable to interact with the RISC in order to promote gene silencing. Thus, the reduction of disulfide bond between MAP and polyplex was shown to be important for siRNA release.

MAP was confirmed to be a powerful CPP for enhanced cellular uptake.[40] We have demonstrated that it is just as impressive when conjugated to a siRNA polyplex. In order to further support its importance, different amounts of MAP were conjugated to the polyplex. The 1:1 CPP/PDP MAP−polyplex had significantly greater uptake (Figure 7a) and activity (Figure 7b) compared with 0.5:1 CPP/PDP MAP−polyplex. Moreover, the conjugation between the two moieties was also a critical factor because when they were incubated together unconjugated, no uptake or activity was observed (Figure 7a, b). Optimizing the amount of MAP on the polyplex was an important consideration because the conjugation of MAP to the polyplex was essential for siRNA cellular uptake and activity. We also demonstrated that MAP mixed with siRNA alone at the same concentrations used for MAP−polyplex preparation could not induce a silencing effect (Figure 6b). Therefore, K21-PDP and MAP were both necessary to achieve a significant knockdown of the target gene, where the former formed a polyplex with siRNA, and the latter delivered siRNA intracellularly without being compromised by any siRNA neutralizing effects. Furthermore, there was no significant difference in the transfection efficiency of the MAP−polyplex

when using Huh7.5 complete medium (containing 10% FBS) or OptiMEM (serum-free) for transfections (Figure 6c). The design of MAP−polyplex presents a platform for conjugation of other targeting or functional moieties, which makes it a promising vehicle for delivery of therapeutic siRNA.

## AUTHOR INFORMATION

### Corresponding Author

*University of Southern California School of Pharmacy, 1985 Zonal Avenue, PSC 404B, Los Angeles, CA 90033, United States. Phone: (323)-442-1902. Fax: (323)-442-1390. E-mail: weishen@pharmacy.usc.edu.

## ACKNOWLEDGMENTS

This research was supported in part by NIH GM070777 (W.-C.S.). We thank Dr. Charles M. Rice, Rockefeller University, and Dr. Jing-Hsiung James Ou, USC School of Medicine, for providing us with the Huh7.5 cells, and Dr. Bangyan L. Stiles, USC School of Pharmacy, for providing us with the PTEN reagents. We also thank Ni Zeng for her assistance with the PTEN silencing assays. R.H.M. is a recipient of the American Foundation for Pharmaceutical Education Predoctoral Fellowship. W.-C.S. is John A. Biles Professor in Pharmaceutical Sciences.

## REFERENCES

(1) Aagaard, L.; Rossi, J. J. RNAi therapeutics: principles, prospects and challenges. *Adv. Drug Delivery Rev.* **2007**, *59*, 75−86.
(2) Elbashir, S. M.; Harborth, J.; Weber, K.; Tuschl, T. Analysis of gene function in somatic mammalian cells using small interfering RNAs. *Methods* **2002**, *26*, 199−213.
(3) Pascual, G.; Fong, A. L.; Ogawa, S.; Gamliel, A.; Li, A. C.; et al. A SUMOylation-dependent pathway mediates transrepression of inflammatory response genes by PPAR-gamma. *Nature* **2005**, *437*, 759−63.
(4) Xie, F. Y.; Woodle, M. C.; Lu, P. Y. Harnessing in vivo siRNA delivery for drug discovery and therapeutic development. *Drug Discovery Today* **2006**, *11*, 67−73.
(5) Meade, B. R.; Dowdy, S. F. Exogenous siRNA delivery using peptide transduction domains/cell penetrating peptides. *Adv. Drug Delivery Rev.* **2007**, *59*, 134−40.
(6) Stevenson, M.; Ramos-Perez, V.; Singh, S.; Soliman, M.; Preece, J. A.; et al. Delivery of siRNA mediated by histidine-containing reducible polycations. *J. Controlled Release* **2008**, *130*, 46−56.
(7) Dalby, B.; Cates, S.; Harris, A.; Ohki, E. C.; Tilkins, M. L.; et al. Advanced transfection with Lipofectamine 2000 reagent: primary neurons, siRNA, and high-throughput applications. *Methods* **2004**, *33*, 95−103.
(8) Park, J. S.; Surendran, S.; Kamendulis, L. M.; Morral, N. Comparative nucleic acid transfection efficacy in primary hepatocytes for gene silencing and functional studies. *BMC Res. Notes* **2011**, *4*, 8.
(9) McNaughton, B. R.; Cronican, J. J.; Thompson, D. B.; Liu, D. R. Mammalian cell penetration, siRNA transfection, and DNA transfection by supercharged proteins. *Proc. Natl. Acad. Sci. U.S.A.* **2009**, *106*, 6111−6.
(10) Man, N.; Chen, Y.; Zheng, F.; Zhou, W.; Wen, L. P. Induction of genuine autophagy by cationic lipids in mammalian cells. *Autophagy* **2010**, *6*, 449−454.
(11) Mo, R. H.; Zaro, J. L.; Ou, J. H.; Shen, W. C. Effects of Lipofectamine 2000/siRNA Complexes on Autophagy in Hepatoma Cells. *Mol. Biotechnol.* **2011**, DOI: 10.1007/s12033-011-9422-6.
(12) Akhtar, S.; Benter, I. F. Nonviral delivery of synthetic siRNAs in vivo. *J. Clin. Invest.* **2007**, *117*, 3623−32.
(13) Whitehead, K. A.; Langer, R.; Anderson, D. G. Knocking down barriers: advances in siRNA delivery. *Nat. Rev. Drug Discovery* **2009**, *8*, 129−38.
(14) Yuan, X.; Naguib, S.; Wu, Z. Recent advances of siRNA delivery by nanoparticles. *Expert Opin. Drug Delivery* **2011**, *8*, 521−36.
(15) David, S.; Pitard, B.; Benoit, J. P.; Passirani, C. Non-viral nanosystems for systemic siRNA delivery. *Pharmacol. Res.* **2010**, *62*, 100−14.
(16) Veldhoen, S.; Laufer, S. D.; Trampe, A.; Restle, T. Cellular delivery of small interfering RNA by a non-covalently attached cell-penetrating peptide: quantitative analysis of uptake and biological effect. *Nucleic Acids Res.* **2006**, *34*, 6561−73.
(17) Chiu, Y. L.; Ali, A.; Chu, C. Y.; Cao, H.; Rana, T. M. Visualizing a correlation between siRNA localization, cellular uptake, and RNAi in living cells. *Chem Biol.* **2004**, *11*, 1165−75.
(18) Muratovska, A.; Eccles, M. R. Conjugate for efficient delivery of short interfering RNA (siRNA) into mammalian cells. *FEBS Lett.* **2004**, *558*, 63−8.
(19) Crombez, L.; Aldrian-Herrada, G.; Konate, K.; Nguyen, Q. N.; McMaster, G. K.; et al. A new potent secondary amphipathic cell-penetrating peptide for siRNA delivery into mammalian cells. *Mol. Ther.* **2009**, *17*, 95−103.
(20) Lundberg, P.; El-Andaloussi, S.; Sutlu, T.; Johansson, H.; Langel, U. Delivery of short interfering RNA using endosomolytic cell-penetrating peptides. *FASEB J.* **2007**, *21*, 2664−71.
(21) Fei, L.; Ren, L.; Zaro, J. L.; Shen, W. C. The influence of net charge and charge distribution on cellular uptake and cytosolic localization of arginine-rich peptides. *J. Drug Targeting* **2011**, *19*, 675−80.
(22) Medarova, Z.; Kumar, M.; Ng, S. W.; Yang, J.; Barteneva, N.; et al. Multifunctional magnetic nanocarriers for image-tagged SiRNA delivery to intact pancreatic islets. *Transplantation* **2008**, *86*, 1170−7.
(23) Zhao, M.; Yang, H.; Jiang, X.; Zhou, W.; Zhu, B.; et al. Lipofectamine RNAiMAX: an efficient siRNA transfection reagent in human embryonic stem cells. *Mol. Biotechnol.* **2008**, *40*, 19−26.
(24) Sashidhar, R. B.; Capoor, A. K.; Ramana, D. Quantitation of epsilon-amino group using amino acids as reference standards by trinitrobenzene sulfonic acid. A simple spectrophotometric method for the estimation of hapten to carrier protein ratio. *J. Immunol. Methods* **1994**, *167*, 121−7.
(25) Smith, R. E.; MacQuarrie, R. A sensitive fluorometric method for the determination of arginine using 9,10-phenanthrenequinone. *Anal. Biochem.* **1978**, *90*, 246−55.
(26) Barnes, M. P.; Shen, W. C. Disulfide and thioether linked cytochrome c-oligoarginine conjugates in HeLa cells. *Int. J. Pharm.* **2009**, *369*, 79−84.
(27) Sir, D.; Chen, W. L.; Choi, J.; Wakita, T.; Yen, T. S.; et al. Induction of incomplete autophagic response by hepatitis C virus via the unfolded protein response. *Hepatology* **2008**, *48*, 1054−61.
(28) Cole, S. P. Rapid chemosensitivity testing of human lung tumor cells using the MTT assay. *Cancer Chemother. Pharmacol.* **1986**, *17*, 259−63.
(29) Sonoda, S.; Schlamowitz, M. Studies of 125I trace labeling of immunoglobulin G by chloramine-T. *Immunochemistry* **1970**, *7*, 885−98.
(30) Read, M. L.; Bremner, K. H.; Oupicky, D.; Green, N. K.; Searle, P. F.; et al. Vectors based on reducible polycations facilitate intracellular release of nucleic acids. *J. Gene Med.* **2003**, *5*, 232−45.
(31) Read, M. L.; Etrych, T.; Ulbrich, K.; Seymour, L. W. Characterisation of the binding interaction between poly(L-lysine) and DNA using the fluorescamine assay in the preparation of non-viral gene delivery vectors. *FEBS Lett.* **1999**, *461*, 96−100.
(32) Zaro, J. L.; Shen, W. C. Evidence that membrane transduction of oligoarginine does not require vesicle formation. *Exp. Cell Res.* **2005**, *307*, 164−73.
(33) Mitchell, D. J.; Kim, D. T.; Steinman, L.; Fathman, C. G.; Rothbard, J. B. Polyarginine enters cells more efficiently than other polycationic homopolymers. *J. Pept. Res.* **2000**, *56*, 318−25.
(34) Zeng, N., Li, Y., He, L., Xu, X., Galicia, V.,et al. Adaptive Basal Phosphorylation of eIF2alpha Is Responsible for Resistance to Cellular Stress-Induced Cell Death in Pten-Null Hepatocytes. *Mol. Cancer Res.* **2011**, DOI:10.1158/1541-7786.MCR-11-0299.

(35) Stiles, B.; Groszer, M.; Wang, S.; Jiao, J.; Wu, H. PTENless means more. *Dev. Biol.* **2004**, *273*, 175−84.
(36) Gomme, P. T.; McCann, K. B.; Bertolini, J. Transferrin: structure, function and potential therapeutic actions. *Drug Discovery Today* **2005**, *10*, 267−73.
(37) Vargason, J. M.; Szittya, G.; Burgyan, J.; Hall, T. M. Size selective recognition of siRNA by an RNA silencing suppressor. *Cell.* **2003**, *115*, 799−811.
(38) Sherman, M. R.; Moran, M. C.; Tuazon, F. B.; Stevens, Y. W. Structure, dissociation, and proteolysis of mammalian steroid receptors. Multiplicity of glucocorticoid receptor forms and proteolytic enzymes in rat liver and kidney cytosols. *J. Biol. Chem.* **1983**, *258*, 10366−77.
(39) Tanaka, K.; Ii, K.; Ichihara, A.; Waxman, L.; Goldberg, A. L. A high molecular weight protease in the cytosol of rat liver. I. Purification, enzymological properties, and tissue distribution. *J. Biol. Chem.* **1986**, *261*, 15197−203.
(40) Zaro, J. L.; Vekich, J. E.; Tran, T.; Shen, W. C. Nuclear localization of cell-penetrating peptides is dependent on endocytosis rather than cytosolic delivery in CHO cells. *Mol. Pharmaceutics* **2009**, *6*, 337−44.
(41) Bartz, R.; Fan, H.; Zhang, J.; Innocent, N.; Cherrin, C.; et al. Effective siRNA delivery and target mRNA degradation using an amphipathic peptide to facilitate pH-dependent endosomal escape. *Biochem. J.* **2011**, *435*, 475−87.
(42) Langlet-Bertin, B.; Leborgne, C.; Scherman, D.; Bechinger, B.; Mason, A. J.; et al. Design and evaluation of histidine-rich amphipathic peptides for siRNA delivery. *Pharm. Res.* **2010**, *27*, 1426−36.
(43) Meyer, M.; Dohmen, C.; Philipp, A.; Kiener, D.; Maiwald, G.; et al. Synthesis and biological evaluation of a bioresponsive and endosomolytic siRNA-polymer conjugate. *Mol. Pharmaceutics* **2009**, *6*, 752−62.
(44) Davis, M. E. The first targeted delivery of siRNA in humans via a self-assembling, cyclodextrin polymer-based nanoparticle: from concept to clinic. *Mol. Pharmaceutics* **2009**, *6*, 659−68.
(45) Liu, K.; Lu, Y.; Lee, J. K.; Samara, R.; Willenberg, R.; et al. PTEN deletion enhances the regenerative ability of adult corticospinal neurons. *Nat. Neurosci.* **2010**, *13*, 1075−81.
(46) Saito, G.; Swanson, J. A.; Lee, K. D. Drug delivery strategy utilizing conjugation via reversible disulfide linkages: role and site of cellular reducing activities. *Adv. Drug Delivery Rev.* **2003**, *55*, 199−215.